

Hyperspectral-enhanced dark field analysis of individual and collective photo-responsive gold-copper sulfide nanoparticles

Paula Zamora-Perez¹, Beatriz Pelaz², Dionysia Tsoutsis¹, Mahmoud G. Soliman^{3,4}, Wolfgang J. Parak³, Pilar Rivera-Gil^{1,*}

¹ Integrative Biomedical Materials and Nanomedicine Lab, Department of Experimental and Health Sciences (DCEXS), Pompeu Fabra University (UPF), Biomedical Research Park (PRBB), carrer Doctor Aiguader 88, 08003 Barcelona, Spain

² Centro Singular de Investigación en Química Biolóxica e Materiais Moleculares (CIQUS), and Departamento de Química Inorgánica, Universidade de Santiago de Compostela, Santiago de Compostela, 15782, Spain.

³ Center for Hybrid Nanostructures, Universität Hamburg, 22607 Hamburg, Germany.

⁴ Physics Department, Faculty of Science, Al-Azhar University, Cairo, Egypt.

* Corresponding author: pilar.rivera@upf.edu

SUPPLEMENTARY INFORMATION

INDEX

Section 1: Nanoparticle characterization, phase transfer and stability.

1. Synthesis of Au/CuS nanoparticles (NPs).
2. Surface coating of Au/CuS NPs.
3. Determination of the concentration of Au/CuS NPs.
4. Stability of polymer-coated Au/CuS NPs in phosphate buffered saline (PBS).
5. Characterization of polymer-coated Au/CuS NPs after water transfer procedure.
6. Single-particle characterization of polymer-coated Au/CuS NPs and spectral mapping verification of the spectral libraries (SLs).

Section 2: NP-cell interactions.

1. Cellular uptake of polymer-coated Au/CuS NPs by human triple negative breast cancer (TNBC) cells using confocal laser scanning microscopy (CLSM).
2. Cytotoxicity assay of polymer-coated Au/CuS NPs in human TNBC cells.
3. Photothermal treatment of human TNBC cells.

Section 3: Spectral analysis of polymer-coated Au/CuS NPs in different relevant environments.

1. Hyperspectral enhanced dark field microscopy (HEDFM) set up.
2. HEDFM characterization of the polymer-coated Au/CuS NPs in different media.

Section 4: Spectral changes related to the protein corona formation.

- 1: Single particle analysis of particles with a different degree of agglomeration.
- 2: Study of the spectral features of different agglomerates.

Section 5: Spectral analysis of polymer-coated Au/CuS NPs over time.

Section 6: Spectral mapping of polymer-coated Au/CuS NPs inside human TNBC cells.

1. HEDFM after cell exposure to polymer-coated Au/CuS NPs.
2. Spectral mapping of polymer-coated Au/CuS NPs in human TNBC cells.
3. Verification of the mapping procedure in control cells.

Section 1: NP characterization, phase transference and stability.

1. Synthesis of Au/CuS NPs.

The hydrophobic NPs formed by a 9-nm gold (Au) spherical domain with a 20-nm copper sulfide (CuS) plate were kindly gifted by Huan Wang, Wenhua Li and Zhishan Bo, Department of Chemistry, Beijing Normal University, Beijing, 100875, P. R. China.

2. Surface coating of Au/CuS NPs.

The NPs were transferred to the aqueous phase by the use of an amphiphilic polymer, poly (maleic-alt-anhydride)–graft-dodecylamine (PMA). The modification of the polymer backbone with dodecylamine is previously reported [1]. The quantity of polymer (V_{pol}) needed to cover the NPs was determined by calculating the total area of NPs [nm^2] that needs to be covered, considering that NPs are spheres of *ca.* 25 nm (d_c). So, the required V_{pol} is:

$$V_{pol} = \frac{\pi \cdot d_{eff}^2 \cdot c_{NP} \cdot V_{NP} \cdot R_{p/area}}{c_{polymer}}$$

where d_{eff} corresponds to the effective diameter of the NP, which is defined as the sum of the NP core diameter (d_c) as determined by transmission electron microscopy (TEM), and twice the estimated thickness of the surfactant ($l_{surf} = 1.2 \text{ nm}$; $d_{eff} = d_c + 2 \cdot l_{surf}$). c_{NP} and $c_{polymer}$ correspond to the NP and the PMA monomer concentration, respectively. In average, 39 monomer units built each PMA molecule. The NP concentration was determined via inductively coupled plasma mass spectrometry (ICP-MS) and TEM as explained in the following. $R_{p/area}$ refers to the amount of PMA monomers needed to be added per NP surface area expressed in nm^2 , this value must be adjusted experimentally. For these NPs, the optimum value is 1000.

Experimentally, 1 mL of a solution of Au/CuS NP with a concentration of 70 nM was mixed with 3.32 mL of a solution 0.05 M of PMA. The mixture was further diluted with 5 mL of chloroform and was evaporated until it was dried in the rotavapor, using a low pressure and a high temperature (60 °C) in the water bath. The evaporation occurred slowly, and after the sample was dried 5 mL more of chloroform were added and dried again. After this process the anhydride rings were opened by the addition of sodium borate buffer (SBB) pH 12. After the complete dissolution of the NPs in water, NPs were filtered with a 0.2 μm syringe filter and were cleaned from the empty micelles of polymer by centrifugation at 15000 g for 20 min [1]. The NPs were dispersed in Milli Q water. The centrifugation washing was repeated 3 times. Afterwards the NPs were fully characterized.

To verify the suitability of the cleaning process, inductively coupled plasma mass spectrometry (ICP-MS) was used to determine the content of Au and Cu in the samples during all the modification stages. A clear change in the morphology of the NPs was observed. However, the core@shell structure is still present with the reduction of the CuS domain. In **Table S1** is presented the summary of the Cu/Au ratios obtained by ICP-MS at the different stages: (i) the NPs in chloroform (“Au/CuS”), (ii) NPs after polymer coating procedure (“PMA(Au/CuS)”), and (iii) NPs after their cleaning by centrifugation

and analysis of the fragment of sample that remains in the supernatant (“PMA(Au/CuS) supernatant”).

Sample	Cu/Au
Au/CuS	6.64
PMA(Au/CuS)	3.05
PMA(Au/CuS) supernatant	8.38

Table S1. Cu/Au ratio determined by ICP-MS of NPs before and after the surface coating process.

Clearly, the percentage of Au is much higher in the purified polymer-coated Au/CuS than in the supernatant where in contrast, the content of Cu is higher. The higher ratio of Cu in the supernatant after the polymer coating and cleaning processes confirms the etching of CuS domain.

3. Determination of the concentration of Au/CuS NPs.

After the synthesis, the NPs in chloroform presented a concentric core@shell morphology (see panel “A” from Figure S1). Whereas, after the phase transfer the conformation of the NPs changed to a dumbbell-like structure consequently to the etching of the CuS domain (panel “B”, Figure S1). These two morphologies were considered to determine the molecular weight of the NPs before and after their water

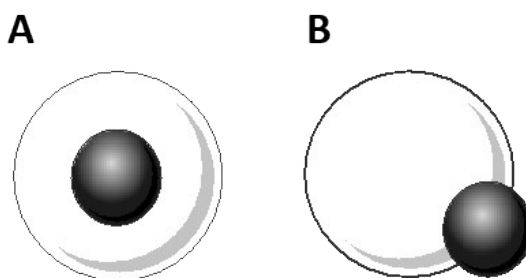


Figure S1. Effect of phase transfer on NPs. Morphological considerations before (A) and after (B) the phase transfer of polymer-coated Au/CuS NPs.

transference (Figure S1).

It was determined from the TEM measurements of the samples in chloroform that the diameter of one NP is ca. 25 nm and the diameter of Au core is ca. 10 nm.

The density of one NP can be calculated determining the volume percentage of Au (4 %) and CuS (96 %) in one NP. As approximation we considered the entire copper sulfide domain as CuS to select the density value. Considering this in **Formula (1)**, we used the following densities values, $\rho_{Au} = 19.3 \text{ g/cm}^3$ and $\rho_{CuS} = 4.76 \text{ g/cm}^3$. The density of Au/CuS NPs ($\rho_{Au@CuS}$) is equal to 5.34 g/cm^3 .

$$\rho_{Au@CuS} = \%Au \cdot \rho_{Au} + \%CuS \cdot \rho_{CuS} \quad (1)$$

To determine the molecular weight of the NPs, first we calculate the volume of a single NP using **Formula (2)**. With this formula we are assuming that the NPs are spherical.

$$V_{NP} = \frac{4}{3} \cdot \pi \cdot \left(\frac{d_c}{2}\right)^3 \quad (2)$$

The molecular weight (M_w) was calculated by following **Formula (3)**:

$$M_w = V_{NP} \cdot \rho_{Au@CuS} \cdot N_A \quad (3)$$

Where, $\rho_{Au@CuS}$ is the density of the NPs and N_A is Avogadro's number. The molecular weight of these NPs is $8.08 \cdot 10^6$ g/mol.

After the phase transfer and considering two spheres, one of Au and one of CuS, the new % of materials were recalculated. The assumption of two spheres was done due to the satellite disposition of the Au NP in most of the NPs after the coating. The Au NP's size was found to be 9.4 ± 1.4 nm and 19.9 ± 2.6 nm the CuS. The %Au is 18.2 and %CuS is 81.76. So, applying "Equation 1" and "Equation 2" the density of polymer-coated Au/CuS NPs is 7.41 g/cm³. So, the molecular weight of the polymer-coated Au/CuS NPs is $2.26 \cdot 10^6$ g/mol. In this case, the "Equation 2" was modified to be considered as the sum of the volumes of two spherical NPs, one of Au and the second of CuS.

ICP-MS measurements were done for different dilutions of sample to determine the inorganic content. The conversion of mass (mg/mL) to molarity can be done using the **Formula (4)**:

$$C = \frac{c}{M_w} \quad (4)$$

Where C is the concentration [M], c is the mass concentration [g/L] and M_w is the molecular weight [g/mol].

Then using a sample with a known concentration (as determined through ICP-MS), extinction spectra were recorded for a dilution series of the sample. The extinction at 450 nm (λ_{450}) was plotted versus the molar concentration. The slope of the regression line corresponds with the molar extinction coefficient at 450 nm. Same approach was applied before and after the water transference (see Figure S2).

The extinction coefficient values are:

Sample	ϵ_{450} [$M^{-1} \text{ cm}^{-1}$]
Au/CuS	$2.88 \cdot 10^7 \pm 1.03 \cdot 10^{-7}$
PMA(Au/CuS)	$7.05 \cdot 10^7 \pm 1.40 \cdot 10^{-7}$

Table S2. Extinction coefficient values before and after water transference procedure.

Notice that the ϵ_{450} in water is higher than in chloroform, we hypothesize that due to the morphological change suffered by the NPs during the water transference some CuS is lost leading to an increase of the Au%. The absorbance of the Au is higher than CuS, so the ϵ value increases.

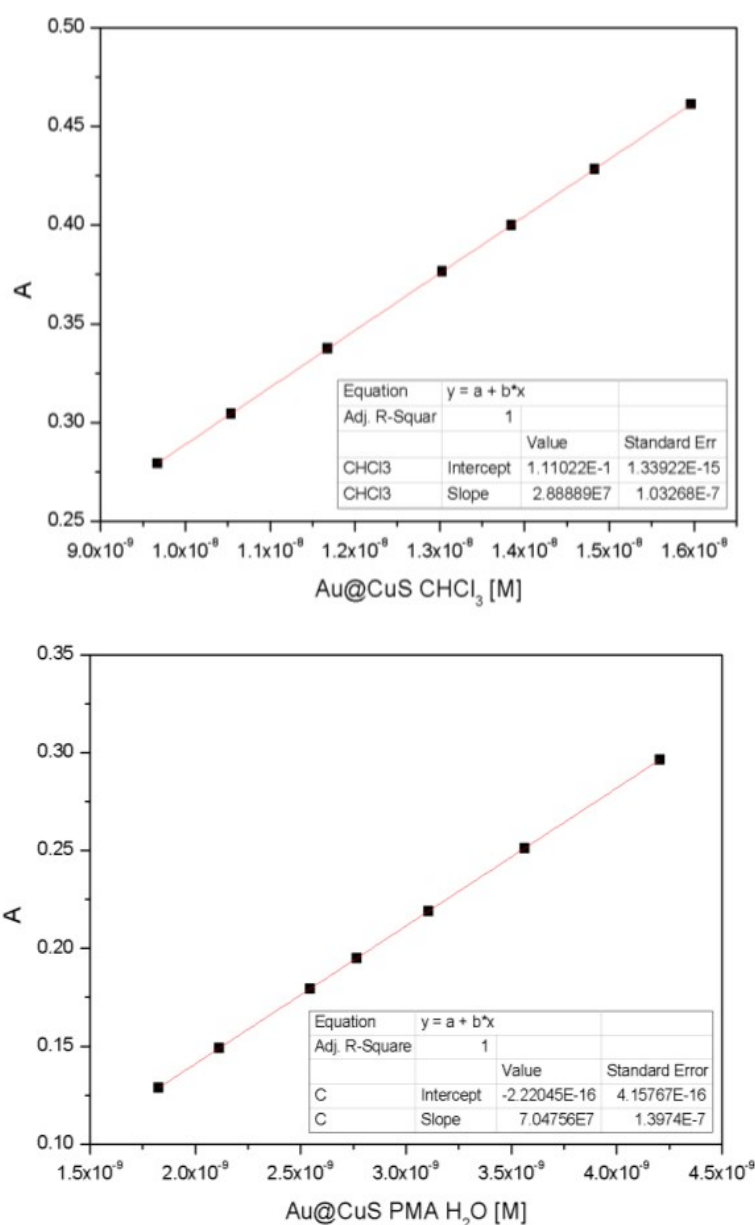


Figure S2. Determination of the molar concentration of Au/CuS NPs. Quantification of the molar extinction coefficient at λ_{450} of the hydrophobic (top) and water-soluble polymer-coated Au/CuS NPs (bottom).

4. Stability of polymer-coated Au/CuS NPs in PBS.

After performing the polymer coating, the stability of NPs over time in PBS 1x was investigated. PBS is a solution with high ionic strength (140 mM NaCl). The monitoring of the extinction spectra with UV-visible spectroscopy along the time was tested by measuring the NPs at different times (see Figure S3) up to 4 d. The absence of variation in the extinction spectra of NPs in PBS indicates that NPs remain unaltered by the high ionic strength and stable with the time in this solution.

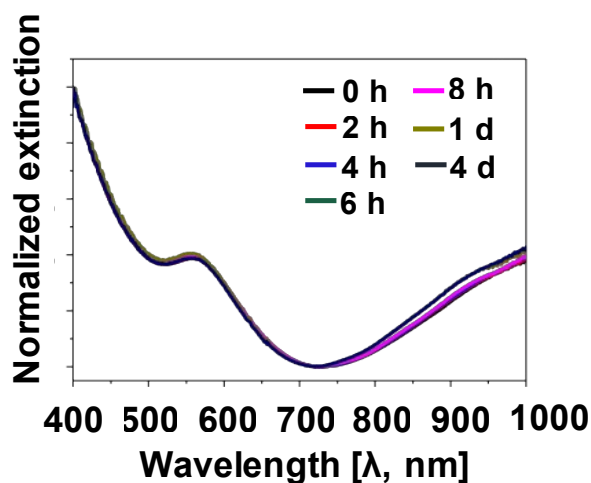


Figure S3. Stability of polymer-coated Au/CuS NPs over time. Normalized extinction spectra of NPs in PBS at 0, 2, 4, 6 and 8 h and 1 and 4 d.

5. Characterization of polymer-coated Au/CuS NPs after water transfer procedure.

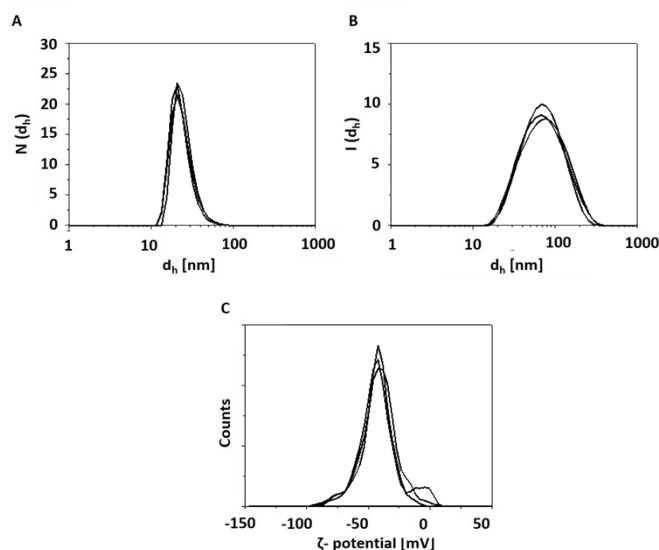


Figure S4. Characterization of polymer-coated Au/CuS NPs in solution. Hydrodynamic diameters as determined by DLS in (A) number, and (B) intensity. Zeta potential graph (C). All the measurements were performed with NPs in water.

Additionally, the hydrodynamic diameter and the ζ -potential were determined (Figure S4) after the water transference process using dynamic light scattering (DLS). The mobility behavior of NPs was also studied by gel electrophoresis with 1% agarose gel and 10 V/cm for 1 h (see Figure S5).

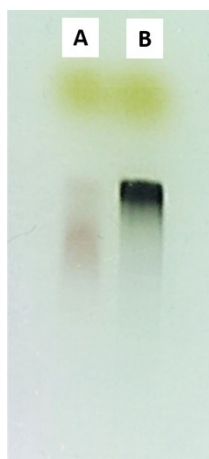


Figure S5. Electrophoretic mobility of polymer-coated Au/CuS NPs. (A) Mobility of phosphine-capped 10 nm Au NPs used as control; (B) Behavior of polymer-coated Au/CuS NPs.

6. Single-particle characterization of polymer-coated Au/CuS NPs and spectral mapping verification of SLs.

The scattering properties of polymer-coated Au/CuS NPs were studied using HEDFM. Firstly, we observed the similarity between the morphology of the NPs observed by in TEM (Figure 2 of the manuscript) and the pattern of colors of single light spots found in the dark field image (DFI). We observed that the light spots present a red domain with bluish edges (see Figure S6). To better study the light scattering properties, 5 light spots randomly selected from the DFI were analyzed (white squares in Figure S6A). We detected two characteristic spectral patterns, one for the red center (red squares in Figure S6B) and the other for the bluish boundaries (blue squares in Figure S6B). From the spectral plots framed with red color (left column) we can observe a clear peak with a maximum light scattering intensity between 619 and 646 nm. This peak also observed in the extinction spectrum of NPs might correspond to the Au domain responsible of the electromagnetic field enhancement [2, 3]. On the contrary, the spectral plots on the right (blue frame), present a multipeak band with lower intensity, which may correlate with the thin edges of the CuS nanoplate that might be more efficient at absorbing light than at scattering it. The color of the particles in the DFI is based on the RGB code applied to the light scattering signal of the plotted spectra (blue, green, and red lines).

After single particle analysis, 150 spectra of each spectral signature were randomly collected to build the two spectral libraries, SLs (Figure S7A). Then the spectra from the SL is compared with the spectra in the hyperspectral data cube (HDC) and the identified spectra appear false colored in the mapping image (Figure S7B). As a result, the pattern described above was validated, finding the inner area and the outer area mapped as red and blue pixels, respectively (Figure S7C). The high correlation between the light spots in DFI and pixels mapped demonstrates the relevance of the spectra selected for the SLs.

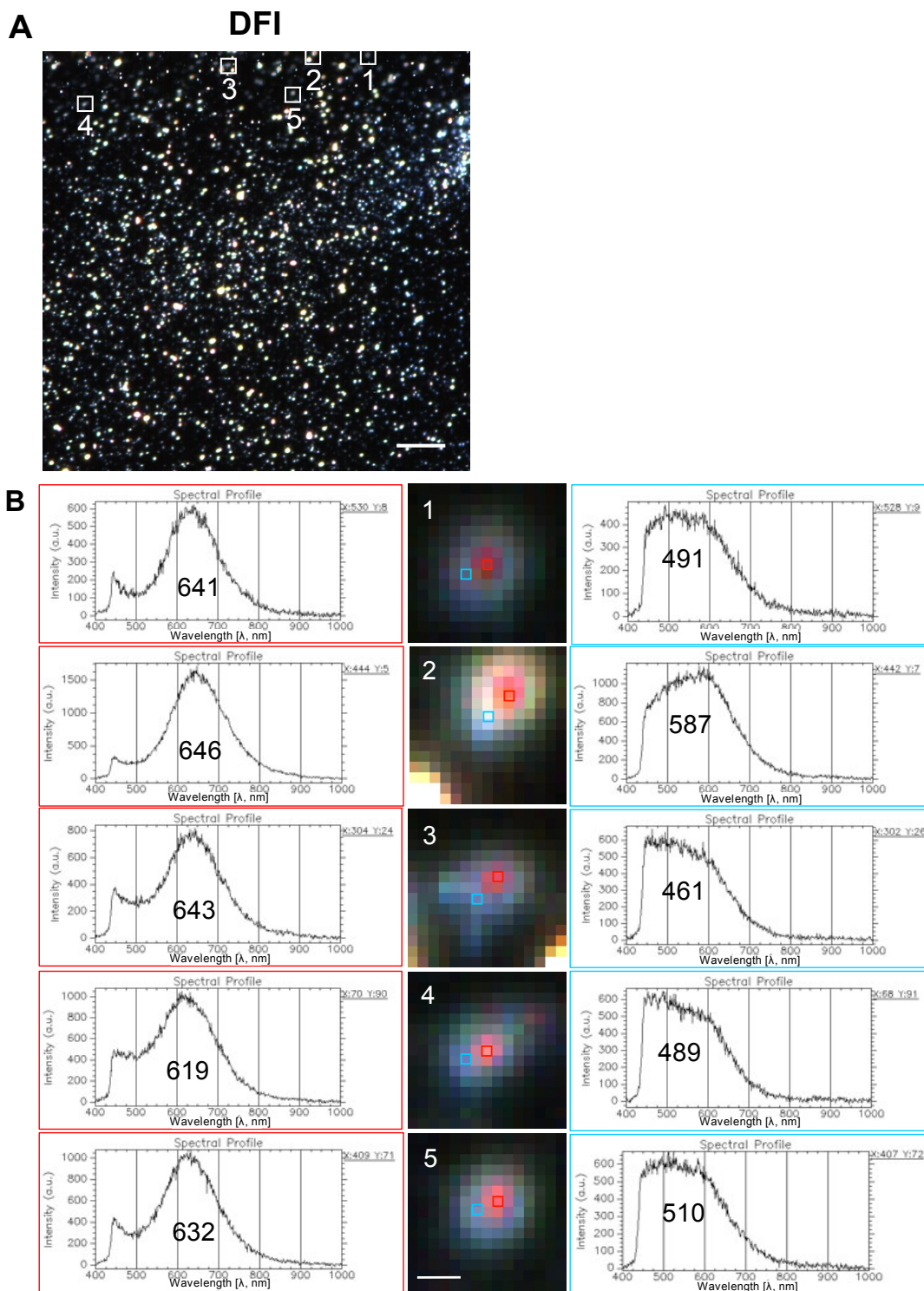


Figure S6. Single particle analysis of polymer-coated Au/CuS NPs. (A) DFI of the particles dispersed in water. The white squares delimit 5 areas randomly chosen. Scale bar: 10 μm ; **(B)** Zoomed areas selected in figure A (1-5) where 5 particles can be observed. It is shown one pixel from the centre (red square) and one from the boundaries (blue square), of each particle. The associated scattering spectra from each pixel it is presented with the same colour code and the wavelength at maximum intensity it is shown. Particle n^o 5 corresponds to the data shown in Figure 2F of the manuscript. Scale bar: 1 μm .

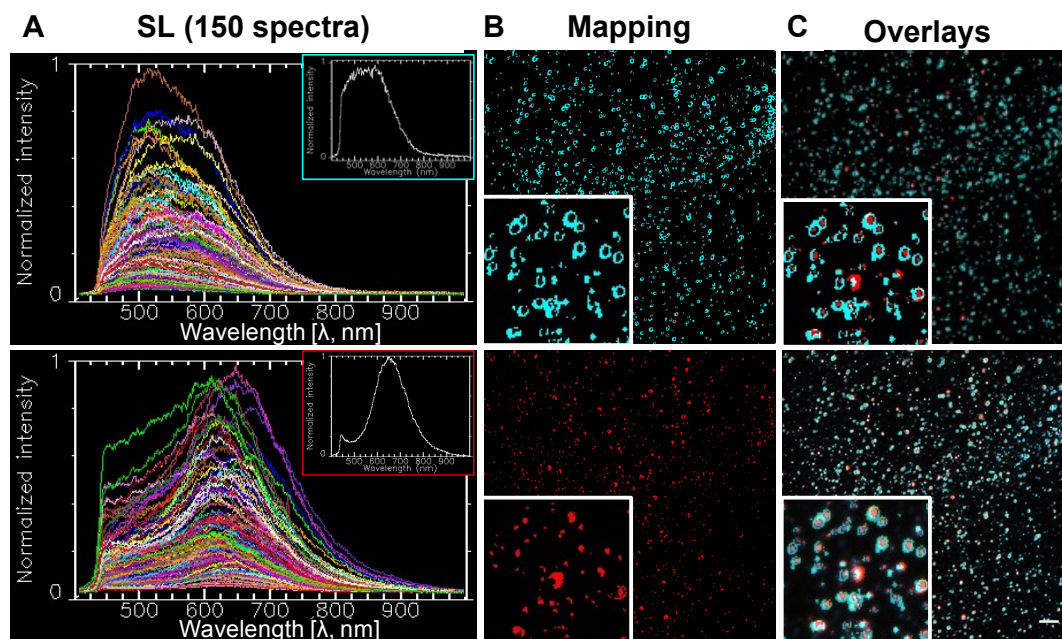


Figure S7. Spectral mapping of the described scattering signatures. (A) SL considering 150 spectra each, of the outer area (top) and the central area (bottom) of polymer-coated Au/CuS NPs scattered light; **(B)** False-colored pixels of identified spectra mapped on the DFI from the outer area (in green) and the central area (in magenta); **(C)** Overlay of the two mapping images (top) and overlay of the merged mappings with the DFI. Scale bar: 10 μm .

Section 2: NP-cell interactions.

1. Cellular uptake of polymer-coated Au/CuS NPs by human TNBC cells using CLSM.

MDA-MB-231 human TNBC cells were seeded onto sterile 12 mm glass coverslips in 6-well plates at 2×10^5 cells/well in cell growth medium (GM) containing 10% fetal bovine serum and incubated for 24 h. After that, 1 μM lysotracker red DND-99 (life technologies, ref. L7528) solution (in PBS 1x) was incubated with 80% confluence cells, for 20 min at 37 $^{\circ}\text{C}$ with 5% CO_2 . Then, a 5-nM polymer-coated Au/CuS NP solution (prepared with GM) was added to the cells and incubated for 3 h. Finally, the 12 mm glass coverslips were placed into glass slides to start scanning with the 543 nm Green Helium-Neon laser, using the 40x 1.25 NA immersion-oil objective of Leica TCS SP2 laser scanning confocal microscope (Leica Microsystems, IL, USA). The overlays generated and the scale bar added to the images were performed using FIJI [4].

In Figure S8 two different controls are provided, cells non-exposed to polymer-coated Au/CuS NPs: (i) without lysotracker showing lack of red signal from cell autofluorescence and (ii) with the lysosomes fluorescently labelled in red upon lysotracker incubation. Lysosomes are acidic organelles and primary degradation system of the cell. Cells exposed to polymer-coated Au/CuS NPs show dark structures (black spots) in the transmitted light images (insets) compatible with intracellular NPs' accumulation. After 3 h, the NPs co-localize with the lysosomes red-labeled in the fluorescence images (see blue arrows in overlay images of Figure S8). The cell morphology is compatible with healthy cells indicating no toxic response to the concentration of NPs used.

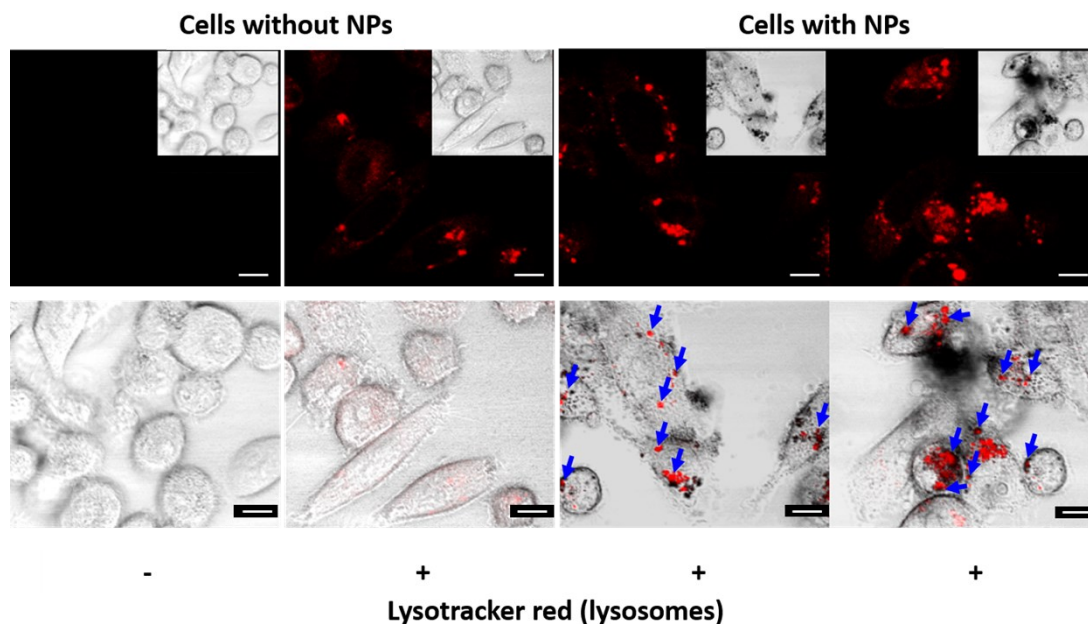


Figure S8. Polymer-coated Au/CuS NPs inside the cells. Intracellular accumulation of NPs (black spots) can be observed inside the lysosomes (red fluorescently labelled) of MDA-MB-231 human TNBC cells, after 3 h of incubation (blue arrows). Scale bar: 10 μm .

2. Cytotoxicity assay of polymer-coated Au/CuS NPs in TNBC cells.

Different concentrations of polymer-coated Au/CuS NPs were tested on MDA-MB-231 human TNBC cells to check their cytotoxicity. Cells were incubated at 37°C with 5% CO₂ for 24 h before the incubation of NPs in a clear-bottom-96-well plate. After that, different concentrations of NPs (100 $\mu\text{L}/\text{well}$) were incubated for 3 h. Then, the tested solutions were discarded and washed with PBS 1x to remove non-internalized NPs. Then, 10% resazurin-based (Sigma Aldrich, ref. TOX8-1kit) solution in GM (100 $\mu\text{L}/\text{well}$) was added to cells and incubated for 3 h. Finally, the fluorescence emission of all tested conditions was read at 585 nm with a Cary Eclipse fluorescence spectrophotometer (Agilent technologies, CA, USA) after exciting the sample at 570 nm with 900 V, 600 nm/min scan rate, 5-nm excitation-emission slits aperture. Each condition tested by triplicate. For the calculations, the fluorescence emission of GM was subtracted to the fluorescence emission of the diverse concentrations of NPs tested and the fluorescence of the samples was normalized to the mean fluorescence of control cells, multiplied by 100 to show the results as a percentage.

3. Photothermal treatment of TNBC.

MDA-MB-231 human TNBC cells were seeded on 35 mm diameter dishes and incubated 24 h at 37 °C, 5% CO₂ in GM. Then, a 15-nM solution of polymer-coated Au/CuS NPs was prepared with GM and placed with the cells for an incubation time of 3 h. Afterwards, the medium was removed to take away the NPs, the cells were rinsed abundantly with PBS 1x, and placed in a solution of 100 μM DAPI (4',6-diamidino-2-phenylindole) in PBS 1x. Immediately after the addition of DAPI (Thermo Scientific, ref. 62248), permeable dead cells were labelled with blue fluorescence and images before and after near-infrared (NIR) laser irradiation were taken (10 min approximately). The blue signal of the

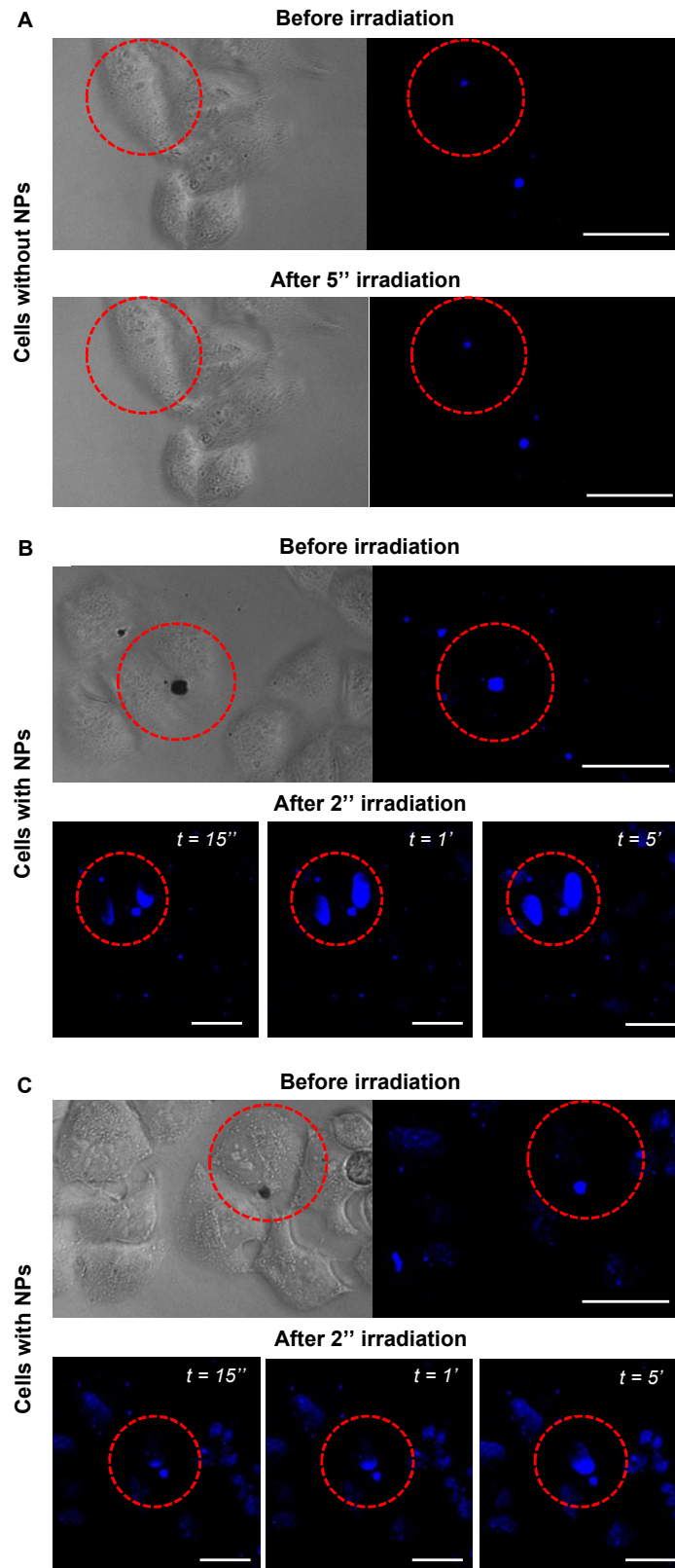


Figure S9. NIR photothermal therapy of MDA-MB-231 human TNBC cancer cells using polymer-coated Au/CuS NPs. (A) Cells non-exposed to NPs before (top) and after (bottom) being irradiated for 5 sec with the therapeutic laser settings (control); the blue fluorescence signal from DAPI does not change with the time meaning that no cell damage was caused; **(B, C)** Cells with internalized polymer-coated Au/CuS NPs before (top) and after (bottom) 2 sec of NIR laser irradiation; Circles show irradiated particles and the increase of blue fluorescence signal of damaged cells over time. Scale bars: 10 μm .

irradiated cells was followed over time to assess the response to the photothermal

treatment (Figure S9B and S9C). Also, non-treated cells were irradiated for 5 sec to discard possible damage caused by laser irradiation itself (Figure S9A).

The microscopy set up consisted in a multiphoton microscopy platform, comprised by a tunable Mai Tai DeepSee (Spectra-Physics) broadband laser emitting at 830 nm (with automated dispersion compensation), connected to an upright Leica TCS SP5 CFS confocal microscope. The maximum average output of the laser at this wavelength is 1.7 W. However, the desired light power reaching the samples using a Leica HCX APO L 40x/0.80 W objective was 140 mW/bleach point laser area.

Cells containing polymer-coated Au/CuS NPs were irradiated at 55% maximum laser intensity (6% gain) during 2-5 sec with the laser irradiation in bleaching point mode. As a control to laser irradiation, cells non-exposed to NPs were treated with the irradiation parameters used for the treated samples. For DAPI fluorescence detection, 405 nm laser line (DAPI channel) was used to excite the samples. DAPI was detected with the PMT at a spectral range between 415-480 nm. In parallel, transmitted light images were obtained.

Section 3: Spectral analysis of polymer-coated Au/CuS NPs in different relevant environments.

▪ HEDFM set up.

The HEDFM imaging system (CytoViva Inc., Auburn, AL, USA) consists on a halogen lamp that supplies white light to the dark field condenser (1.2-1.4 NA, immersion oil; ~400 μ m field of view). Light reaches the sample in an oblique angle passing through the dark field condenser. Then, light is reflected, and the desired light scattering reaches the 60x objective of the Olympus BX43 microscope (1.25-0.65 NA, oil iris). Then, the light arrives to the spectrograph *V10E 2/3"* attached to a scan CCD *Imperx IPX-2M30* camera, which collects the dark field image and the scattering spectra of the sample. The ENVI software, controls the equipment and the sample acquisition. The software collects the light reflected from the sample in a spectral range from 400 to 1000 nm, with a spectral resolution of 2.73 nm, one line at a time. Spatial and spectral data are collected in each pixel in the line. The HDC is generated by compiling pixelated lines into a single image. The series of lines are created in almost 5 min, depending on the exposure time needed for each sample [5].

▪ HEDFM characterization of the polymer-coated Au/CuS NPs in different media.

Polymer-coated Au/CuS NPs were diluted from the 1.08 μ M stock solution in milli Q water to the optimal concentration (> 150 NPs per HDC) using different medium: (i) milli Q water, (ii) PBS 1x (higher ionic strength than water), (iii) GM containing 10% foetal bovine serum proteins at neutral pH (pH 7 simulating cellular fluid), and (iv) GM with pH 4 (simulated lysosomal fluid) tuned with HCl 0.1 M solution. After sonication of the solutions, 5 μ L drop of each sample was placed onto a clean microscope slide covered with a glass coverslip. We waited until NP stabilization for the HDC acquisition. The exposure time used for all the samples was 0.3 ms (see HDCs from Figure S10).

Once the HDC was acquired with the ENVI 4.8 software (Exelis Visual Information Solutions, Boulder, CO, USA), the spectral analysis was done by using different approaches. The lamp spectrum was subtracted from all the spectra considered in this work.

i) Polymer-coated Au/CuS NPs in water (original dispersant).

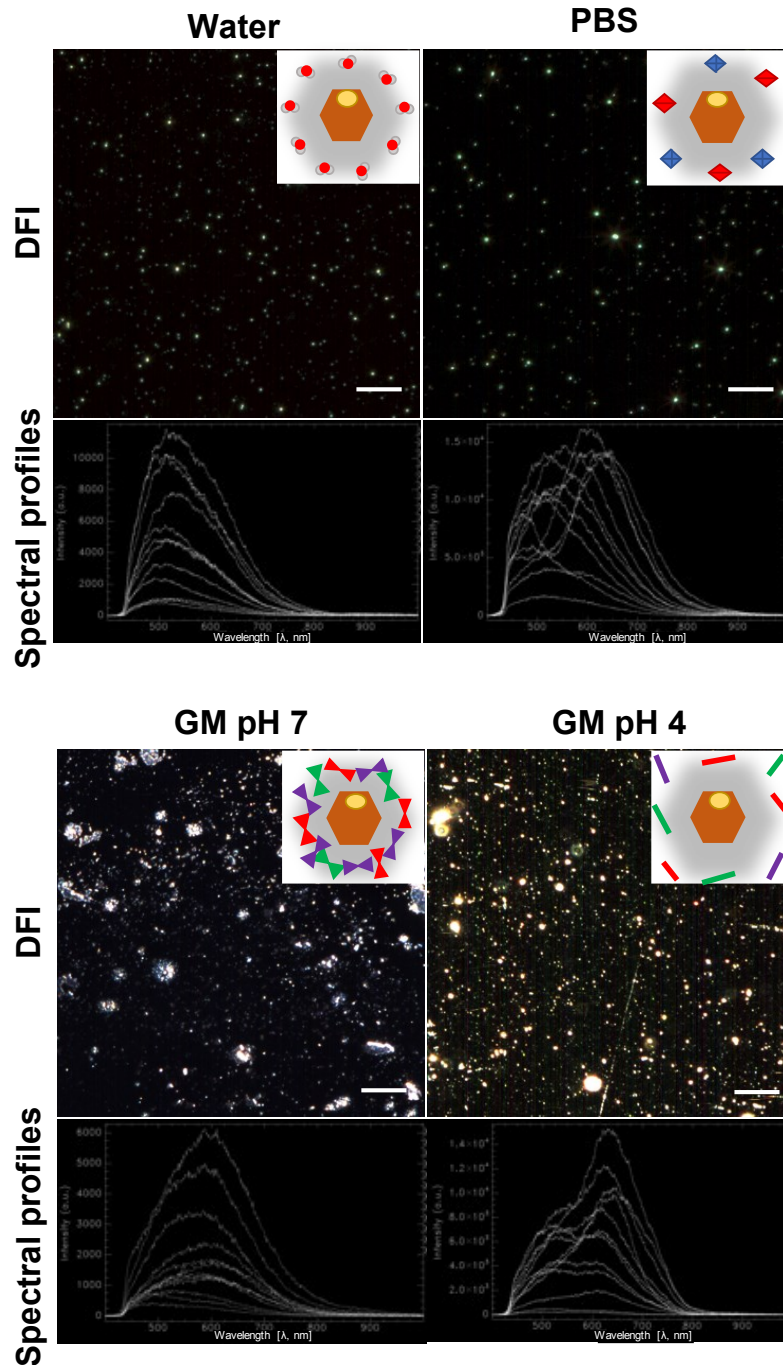


Figure S10. Single spectral behaviour of polymer-coated Au/CuS NPs exposed to different relevant biological environments. The scattering signal of 12 particles randomly selected for water, PBS, neutral GM, and acidic GM conditions. The insets show the solvation of the NPs exposed to water, the salt-interaction when exposed to PBS, the protein corona formation upon protein interaction in neutral GM and the interaction with proteins affected by the acidic pH. In the DFI of polymer-coated Au/CuS NPs exposed to protein media (pH 4 and 7) it can be observed some particle agglomeration/aggregation, whereas in water and PBS this effect is not observed. Scale bar: 10 μm.

The polymer-coated Au/CuS NPs were diluted in milli Q water before the acquisition. The HDC (Figure S10) was analyzed using the particle filtering tool, obtaining a total of 432 particles after removing undesired spectra. This tool recognizes the number of pixels that form each light spot in the DFI coming from the light scattering of NPs and calculates the mean spectral profile of all the pixels contained per particle. The particles can be also classified by their number of pixels and the mean spectral profile of the different subpopulations can be generated. Finally, the NPs can be classified by their number of pixels and the mean spectral profile of the different subpopulations can be generated. The mean spectral profile of all the NPs was calculated and after that, classified regarding their number of pixels into different subpopulations.

- ii) Polymer-coated Au/CuS NPs in PBS (high ionic strength without protein corona).

Polymer-coated Au/CuS NPs were exposed to PBS 1x. After the exposure to a media with a higher ionic strength than water (and without proteins) lack of changes in the solution suggesting agglomeration/aggregation of NPs were observed. 346 particles were detected from the HDC (Figure S10) and the mean spectral profile was obtained.

- iii) Polymer-coated Au/CuS NPs in neutral protein-rich media (extracellular/early endosome conditions with protein corona).

Polymer-coated Au/CuS NPs were placed into GM used for culturing MDA-MB-231 human TNBC cells. The GM contains a 10% of protein content (FBS). These conditions simulate the environmental conditions of the extracellular NPs and the particles that have been internalized but locate in early endocytic vesicles. Upon exposition to proteins an interaction with the surface of the polymer-coated Au/CuS NPs occur, forming the so-called protein corona. The protein corona plays a key role in particle stability being able to drive stabilization as well as agglomeration/aggregation processes. After the acquisition of the HDC (Figure S10), the NPs were filtered by the number of pixels of each light spot, obtaining a total of 706 particles.

- iv) Polymer-coated Au/CuS NPs in acidic protein-rich-media (lysosomal conditions without protein corona).

Polymer-coated Au/CuS NPs were introduced into a pH-4 GM solution to mimic the pH of the intracellular NP conditions in the lysosome and study the related spectral changes. The incubation time of the NPs was the same applied in section 2 for NP-cell interactions. (3 h), where the internalization of polymer-coated Au/CuS NPs was confirmed. The HDC (Figure S10) was analyzed using the particle filtering tool, obtaining 590 particles after removing undesired spectra. The mean spectral profile of all the NPs was obtained and then, the particles were classified regarding their number of pixels forming the light spots. The lamp spectrum was subtracted from the spectral profiles of the NPs. The broadening of the mean spectral profiles it was also studied (see Figure S13.C) by calculating the full wide half maximum being the order as follows, from the broadest to the narrowest: water > GM pH 4 = GM pH 7 > PBS.

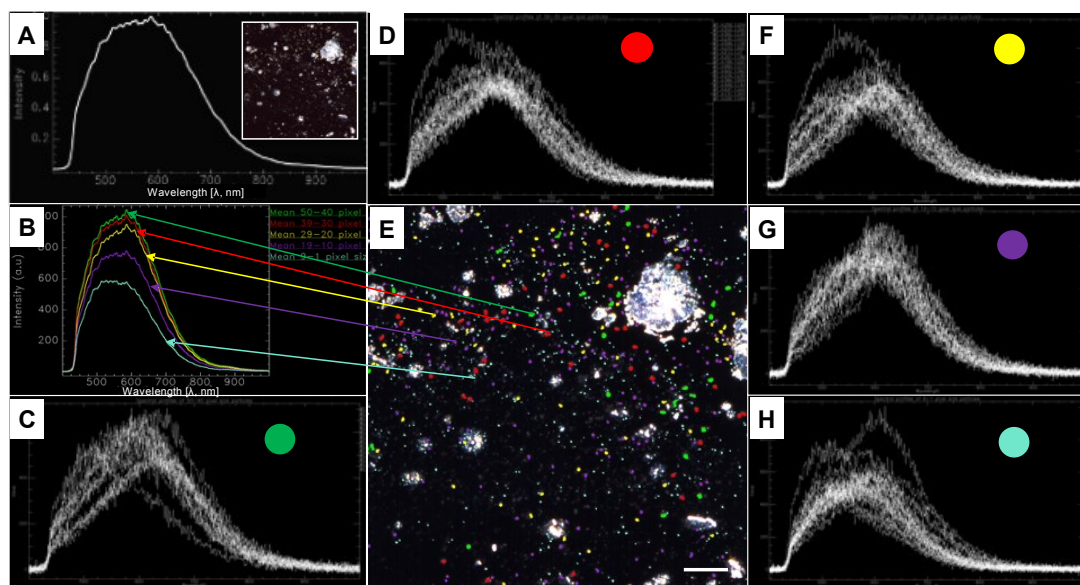


Figure S11. Schematic representation of the workflow followed for the obtention of mean and single spectral profiles from the NPs of interest. (A) Mean spectral profile of all non-agglomerated particles presented in the DFI (inset); (B) Mean spectral profiles of non-agglomerated NPs presented in Figure A, sorted by the size of light spots. (E) DFI presenting the different subpopulations of light spots sorted by size and identified as false-colored ROIs using the particle filtering tool. Each subpopulation is labelled with a color. The arrows present the relationship of ROIs with the spectra shown in Figure B. The mean spectral profiles contain the spectral information false-colored in the DFI. To track the information, the same color code was used. (C, D, F, G, H) Single spectra from each subpopulation (following the color of the ROIs) were randomly collected from the particle filtering tool. The plots show the intra/interparticle variability of the optical response.

After acquisition of the NPs in the four different environmental conditions, 12 randomly selected spectra were plotted to show the intraparticle and interparticle variability (Figure S10). Then, the NPs identified and sorted by their number of pixels using the particle filtering software tool, were exported as ROIs and false-colored for an easy identification of the different NP subpopulations (see scheme on Figure S11). All the spectra considered in the particle filtering process can be also used for the creation of SLs. After merging all the ROIs, the mean spectral profile of the overall particles can be obtained (Figure S11A). The comparison of the mean spectral profiles of the diverse subpopulations exposed to different media is provided in Figure S12 and S13 and explained in the manuscript.

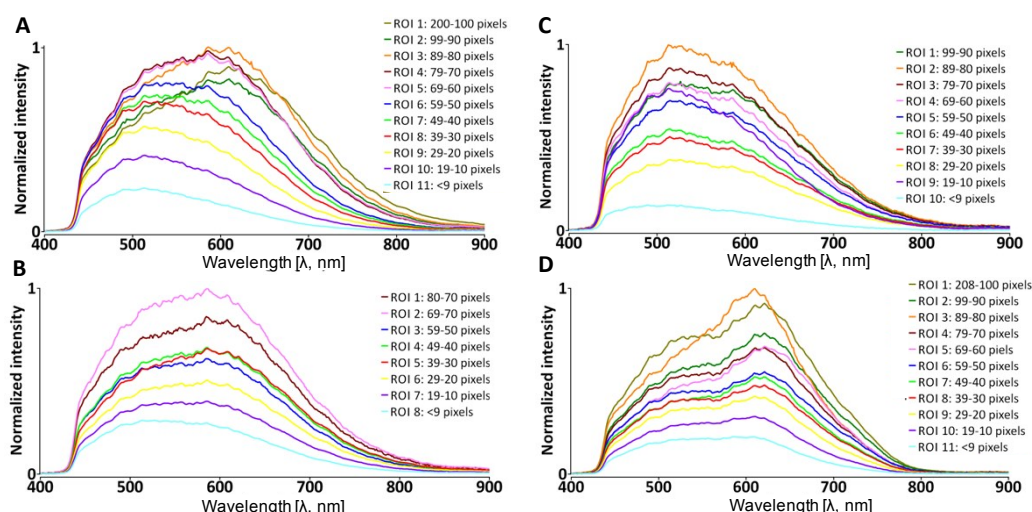


Figure S12. Mean spectral analysis of the subpopulations of polymer-coated Au/CuS NPs exposed to different biological media. Mean spectral profiles of NPs exposed to (A) water, (B) GM at pH 7, (C) PBS 1x, and (D) GM at pH 4, sorted by size (number of pixels) in different ROIs. Each subpopulation (ROI) presents a specific colour throughout all the environments. The similarity of the spectra is higher for the particles exposed to water and neutral GM than for water and PBS or acidic GM.

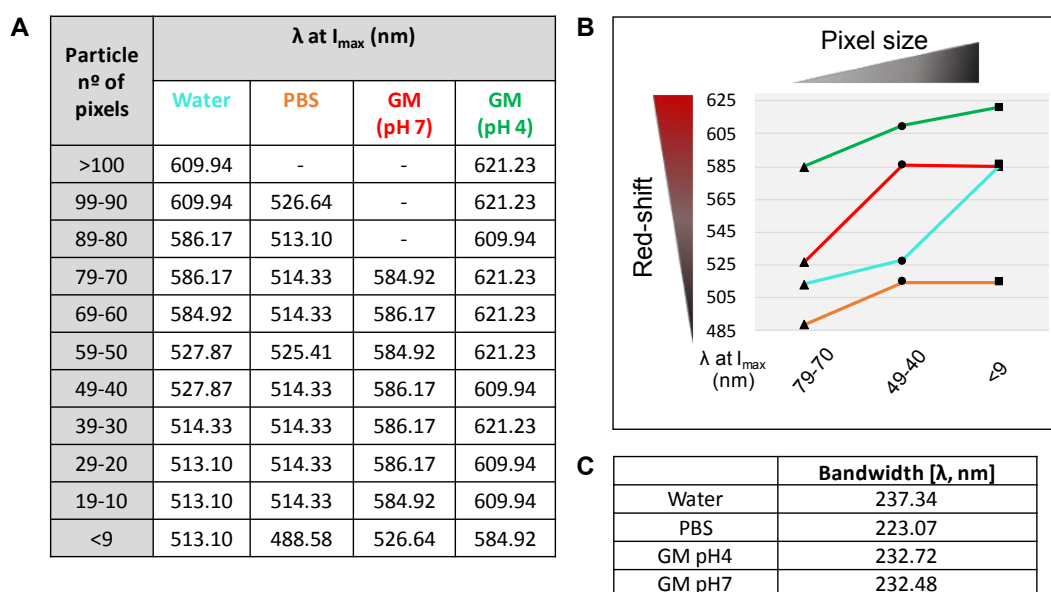


Figure S13. Analysis of the wavelength at maximum intensity of polymer-coated Au/CuS NPs in different media. (A) Table with the wavelengths of the maximum light scattering intensity of the mean spectral profiles of the particles exposed to different media sorted by the number of pixels; (B) Graph showing the relationship between the number of pixels of the particles: in water (blue), PBS (orange), neutral GM (red) and acidic GM (green), and the redshift of the maximum λ light scattering wavelength. The three different points plotted correspond to particles with different number of pixels, presented in A; (C) Bandwidth of the mean spectral profiles of water, PBS, GM pH 4 and GM pH 7.

Section 4: Spectral changes related to the protein corona formation.

The agglomerates of particles observed in the sample exposed to protein rich environment (GM pH 7) which were not included in the previous particle filtering procedure (Figure 4, S12 and S13), are evaluated in this section.

1. Single particle analysis of particles with a different degree of agglomeration.

Using the original HDCs, we studied the behavior of polymer-coated Au/CuS NPs in presence of the protein corona. Figure S14.A shows the differences in bandwidth of the mean spectral profiles presented in Figure 5 (“ROIs 1-4”). The bandwidth was calculated at the half maximum intensity for comparison. Particles with different agglomeration status were also studied in Figure S14B for a single pixel spectral evaluation. A particle from an agglomerate observed in GM pH 7 (Figure S14B, “ROI 1”) and a primary particle (Figure S14B, “ROI 2”) were analyzed and compared with primary particles exposed to acidic GM (Figure S14B, “ROI 3”) and PBS 1x without protein corona (Figure S14B, “ROI 4”). All the particles were randomly selected. The spectra of the particle from the agglomerate (indicated with a white arrow) display broader bands and prominent contribution in the 600-900 nm range in comparison to the primary particles. The change in the optical response of agglomerated particles can be explained as the higher degree of interparticle interaction, the more heterogeneous is the electron resonance and the optical response. The scattering spectral response between the primary particles in neutral GM (“ROI 2”) and PBS (“ROI 4”) does not vary dramatically (peaks

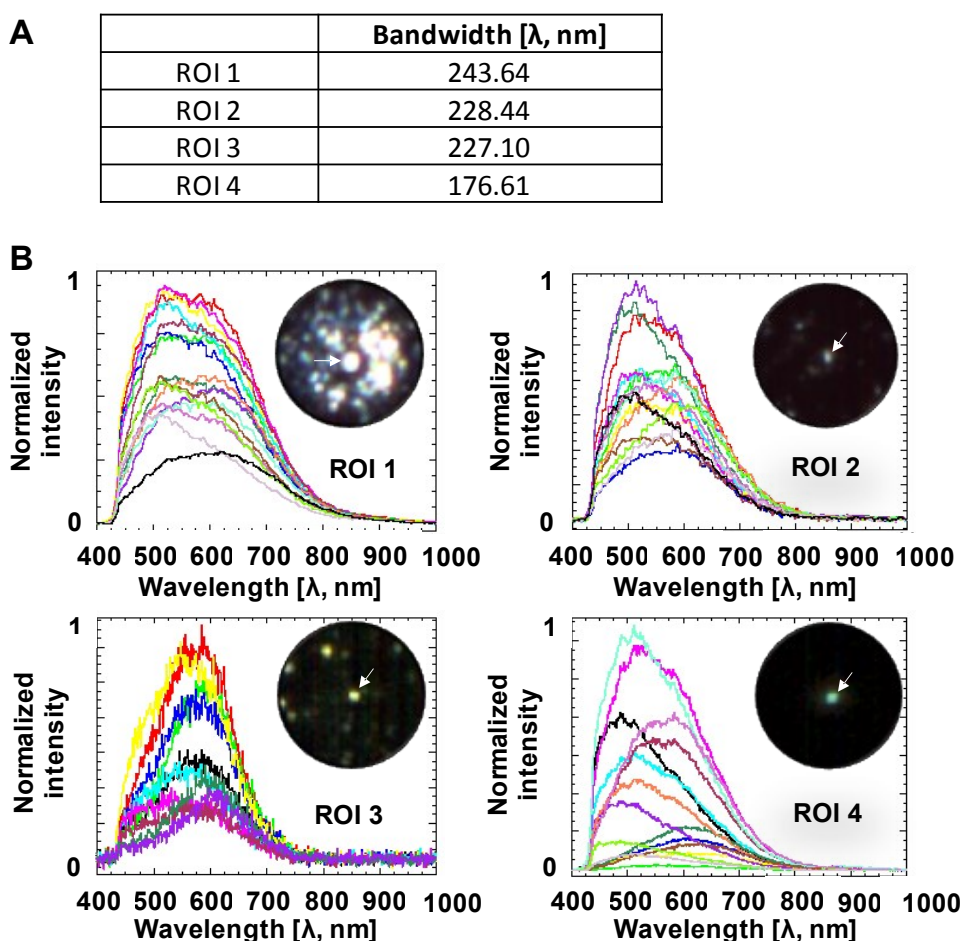


Figure S14. Spectral analysis of polymer-coated Au/CuS NPs in different cellular environments. (A) Calculations of the bandwidth for the different mean spectral profiles studied in Figure 5 (ROIs 1-4) (B) Individual spectra obtained from NPs contemplated in Figure 5, ROIs 1-4. In Figure 5 the mean spectra are plotted whereas this figure shows the spectral profile of individual pixels ($n = 16$) taken from the areas labelled with the arrows in the DFI.

around 512 nm). The blue contribution is more prominent for spectra in “ROI 2”, as it can be seen from the DFI where the particle looks blue while the particle in “ROI 4” looks greener. In contrast, the spectral behavior of the particle in acidic GM (“ROI 3”) differs from the rest of particles, appearing yellow (peak around 575 nm) in DFI.

2. Study of the spectral features of different agglomerates.

Ten of the agglomerates observed in the protein rich environment (“GM pH 7”) were identified and classified as different ROIs, numbered from 1 to 10. The ROIs false colored in the DFI are depicted in Figure S15A, while the mean spectral profiles and the band maximum of each agglomerate is represented in Figure S15B and S15C. As a result, the spectra presented in Figure S15 show a broaden band typical from agglomerated/aggregated particles. The agglomerates with higher relative intensity (“ROI 7” and “ROI 8”) display the band maximum intensity at 586 and 591 nm, respectively. Nevertheless, ROIs 1 and 10 that are two of the agglomerates with lower intensity, present the band maximum at 513 and 514 nm, respectively. Closer particle interplay drives an enhanced electromagnetic interaction, favoring the scattering performance of polymer-coated Au/CuS NPs. In Figure S16 the agglomerates are deeply examined.

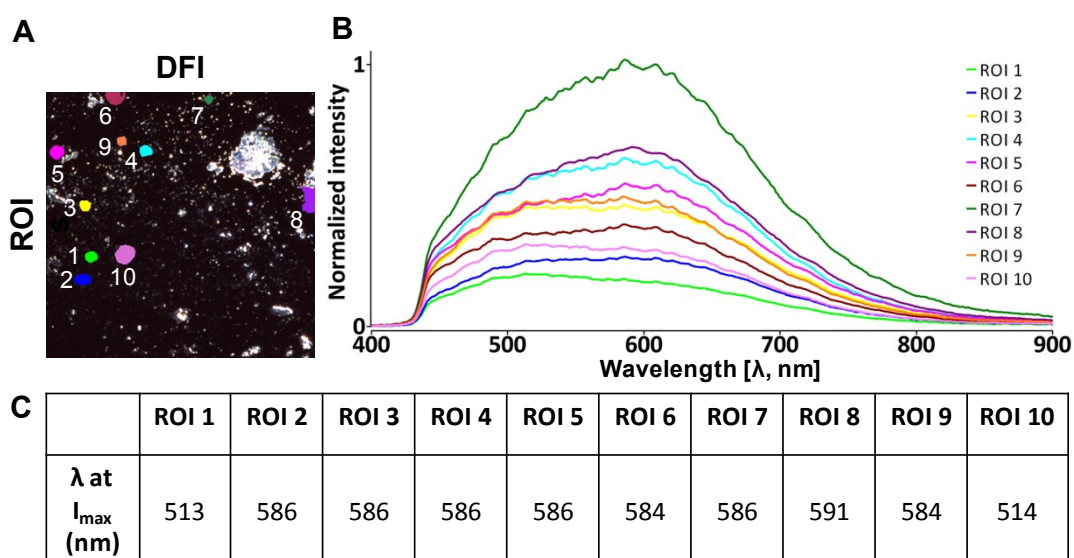


Figure S15. Mean spectral comparison of agglomerates formed upon protein interaction. (A) DFI with false-coloured ROIs showing the agglomerates under study ($n = 10$); (B) Mean spectral profiles obtained from all the spectra contemplated in the pixels defined by the ROIs; (C) Table showing the wavelength of the maximum light scattering of each agglomerate. From the 10 agglomerates, agglomerates 1 and 10 present particles with a lower agglomeration degree.

From each ROI represented in Figure S15, 16 spectra were randomly collected for a single particle analysis (see Figure S16). The maximum scattering intensity spectra were selected for this comparative purpose. In the plots (Figure S16) it can be observed that spectra with lower intensity belong to particles with a smaller number of pixels, which present a blue color in the DFI due to their maximum intensity peak around 512 nm. As the particles present a higher number of pixels, the spectra result in a band broadening, and their maximum light scattering intensity increases and shifts to the NIR (~600 nm).

Comparing the 100 nm redshift of the particles present in the agglomerate with the 58 nm redshift between the primary particles analyzed in Figure S13 and considering the classical DLVO theory, we confirm the higher agglomeration status of the particles upon protein interaction as reported in other studies [6, 7].

Section 5: Spectral analysis of polymer-coated Au/CuS NPs over time.

1. Spectral changes of NPs over time.

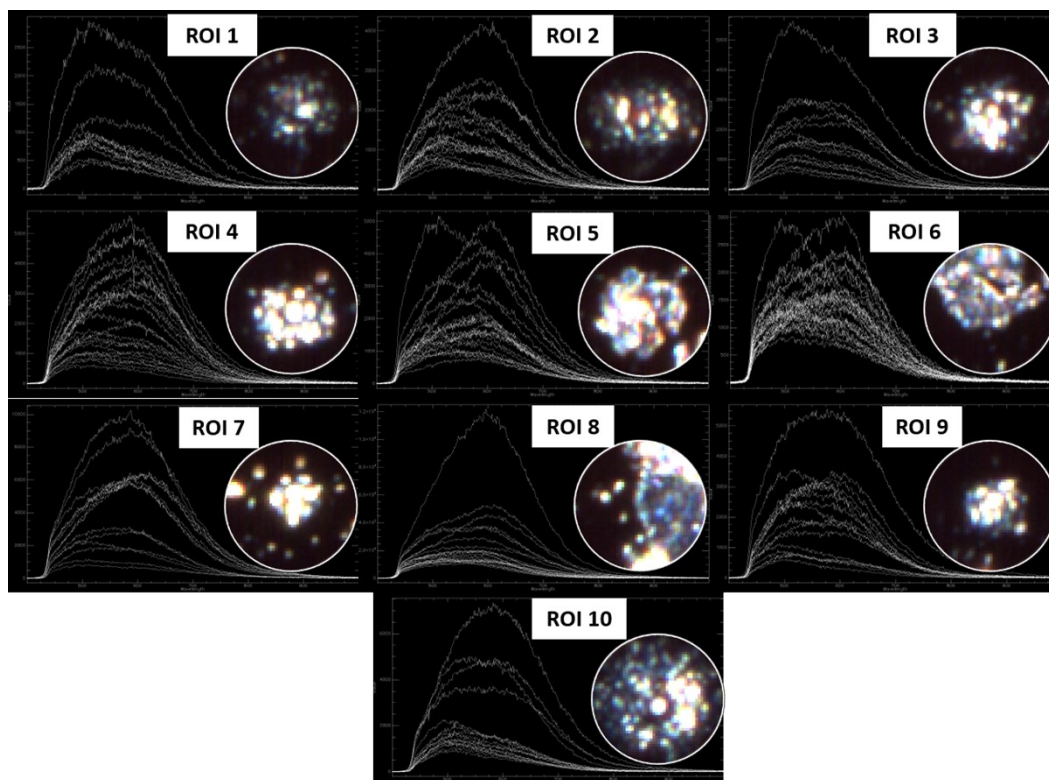


Figure S16. Spectral analysis of 10 agglomerates of polymer-coated Au/CuS NPs formed upon protein interaction. Plots present the scattering spectra of 15 particles randomly selected per agglomerate. The spectra present the heterogeneous optical response of different agglomerated particles. The primary particles show a blue light scattering in the DFI whereas the more complexed particles exhibit an orange response. The spectral broadening and redshift observed in spectra from each agglomerate are likely resultant from the sum of the scattering contributions of different particles.

Following the same procedure previously explained, HDC of polymer-coated Au/CuS NPs in neutral GM were obtained at different time points: $t = 0$, after 2 months (“ $t = 1$ ”), 5

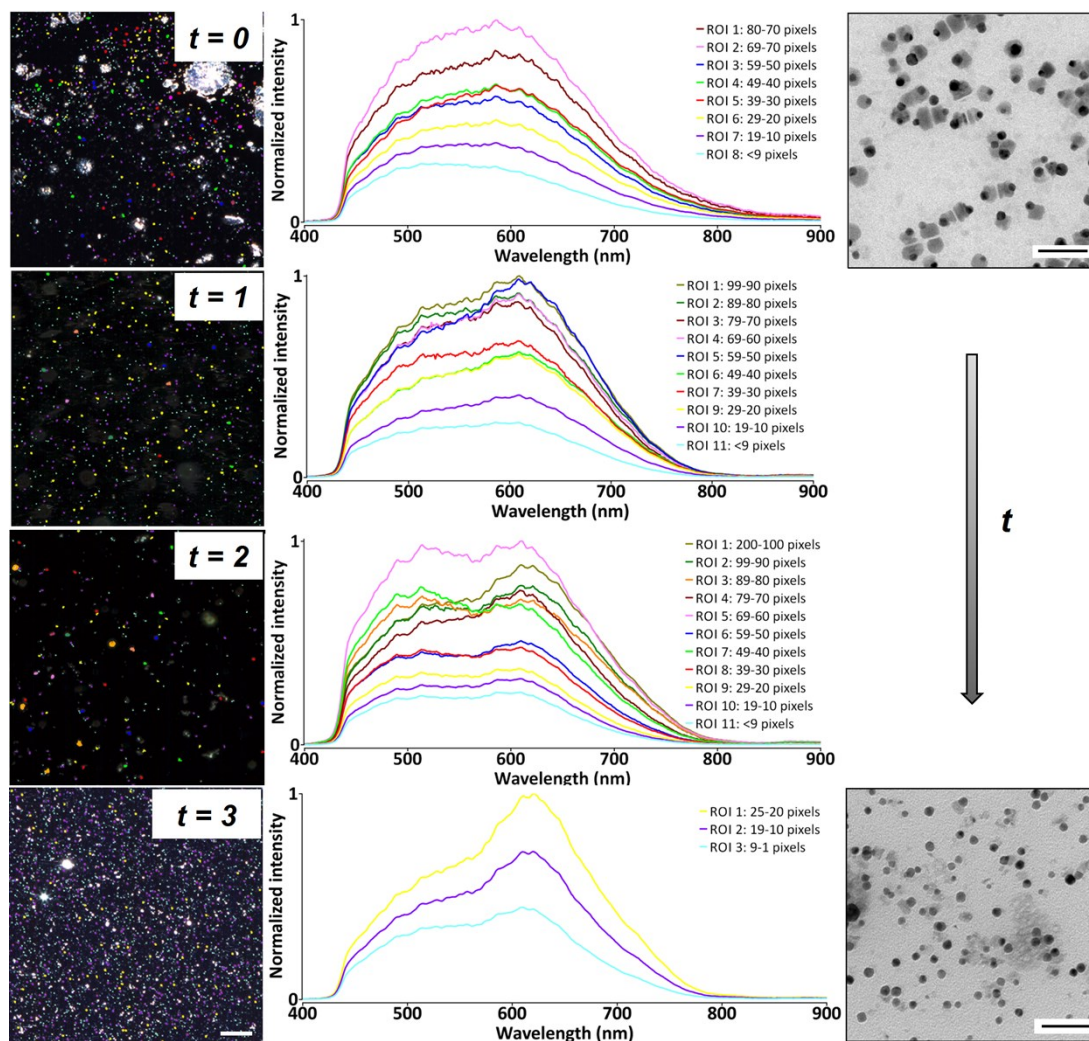


Figure S17. Spectral changes of polymer-coated Au/CuS NPs in GM pH 7 over time. DFIs of the NPs under study at different time points (left column): at $t = 0$, after 2 months ($t = 1$), 5 months ($t = 2$), and 8 months ($t = 3$). The NPs were sorted by their size as light spots (number of pixels) and false coloured as diverse ROIs in the DFIs. Scale bar: 10 μM ; Mean spectral profiles of the different subpopulations sorted by the number of pixels (middle column). The colour of the spectra correlates with the colour of the ROI in the DFI; TEM images showing the morphological changes of polymer-coated Au/CuS NPs after 8 months of exposure to neutral GM (right column). Scale bar: 50 nm.

months (“ $t = 2$ ”) and 8 months (“ $t = 3$ ”), for the investigation of the spectral changes related to particle ageing over time (see Figure S17). Once the HDCs of the samples were performed, the particle filtering analysis was done to collect the spectral profiles of each NP of interest, considering the size of the light spot, in pixels. Then, the spectral information of the NPs was exported as ROIs, and the ROIs related to the same subpopulation were merged to obtain a mean spectral profile of each interval of size (in pixels).

The morphology of the particles was tracked at the beginning (“ $t = 0$ ”) and at the end (“ $t = 3$ ”) of the study by using TEM, to correlate the structural changes with the spectral

differences. The results obtained show a clear particle ageing after 8 months. The TEM

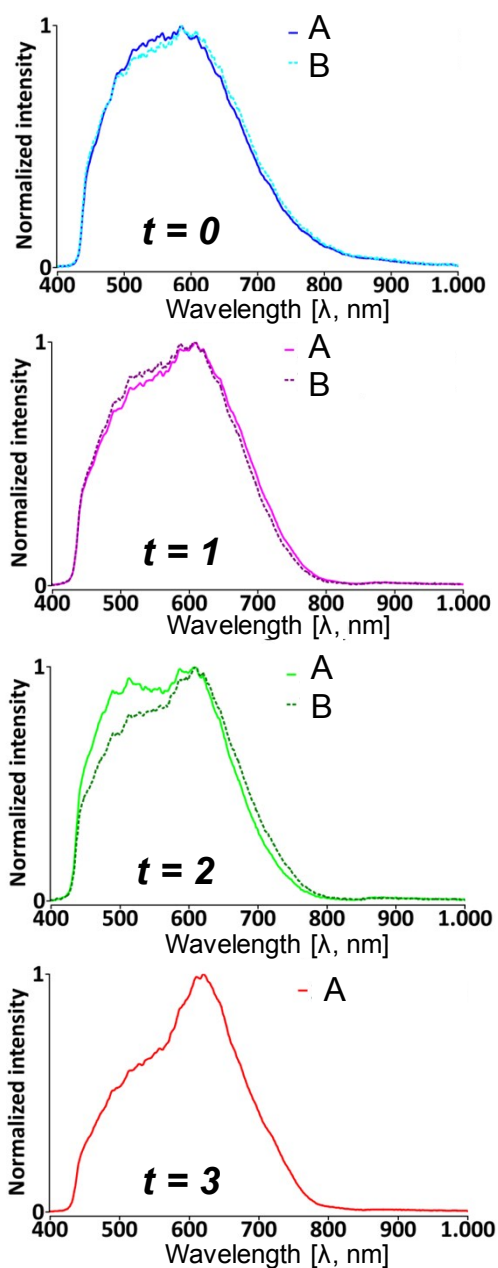


Figure S18. Mean spectral comparison of two subpopulations of polymer-coated Au/CuS NPs with different number of pixels over time. The mean spectral profiles of two subpopulations of light spots with different size are monitored over time at $t = 0$, after 2 months ($t = 1$), 5 months ($t = 2$), and 8 months ($t = 3$). Particle A corresponds to NPs with 20-29 pixels, false-coloured ROIs in yellow at the DFI and particle B corresponds to NPs with 70-79 pixels, false-coloured ROIs in bordeaux in the DFI (see Figure S10). After 8 months, the particles with 80-89 pixels disappeared by degradation of NPs.

images present several gold NPs particles with almost totally disappeared CuS, and very few particles maintaining the original structure but with decreased density in the CuS nanoplate. Therefore, the morphological and compositional changes of polymer-coated Au/CuS NPs over time, are translated into a gradual loss of scattering ability in the spectral range of 450-575 nm. The spectral analysis of the subpopulations (Figure S17) at each time point, reflects a homogeneous response of the particles to different conditions. The distribution and subclassification of the particles can be appreciated in the DFI as false colored ROIs. When comparing two different subpopulations over time (Figure S18), one comprising 20-29 pixels (yellow spectrum and false colored ROIs in DFI) and other 70-79 pixels (bordeaux spectrum and false-colored ROIs in DFI), we can see that the NPs with more pixels exhibit a more evident effect as they were not detected in the last time point. As the light spot size decreases, the bigger subpopulations disappear, and the scattering performance is altered with the time.

Section 6: Spectral mapping of polymer-coated Au/CuS NPs inside human TNBC cells.

1. HEDFM after cell exposure to polymer-coated Au/CuS NPs.

For cell imaging with HEDFM similar procedure used for CLSM experiment was followed. MDA-MB-231 breast cancer cells were seeded onto glass coverslips placed (one by one) into a 6-well plate at 2×10^5 cells/well and incubated for 24 h. Cells were exposed to polymer-coated Au/CuS NPs at 15-nM concentration for 3 h and washed with PBS 1x for non-attached-particle removal. Control cells non-exposed to NPs were also prepared. The HDCs were obtained at 60x objective magnification.

2. Spectral mapping of polymer-coated Au/CuS NPs in human TNBC cells.

The HDC of control cells and cells exposed to polymer-coated Au/CuS NPs were lamp

corrected and resized. After that, an extensive ROI for polymer-coated Au/CuS NPs in

GM pH 7 was manually performed and posteriorly, the ROI was converted in to a SL_{pH7} .

For polymer-coated Au/CuS NPs in GM pH 4, the particle filtering tool was used to obtain

the SL_{pH4}. Then SL₇ and SL₄ were filtered against the HDC of control cells to remove

coincident spectra, using a SAM parameter of 0.1 radians. The resulting SL_7 and SL_4

contained 7704 and 5527 spectra, respectively (HDCs from § 3, “GM pH 7 and 4”), which

were divided in different subsets (Figure S20, "Subset of SL"). After selecting the most

relevant spectra for the mapping, they were tested using the spectral angle mapper

(SAM) parameter of 0.1 radians in the HDC of the cells exposed to polymer-coated

Au/CuS NPs. The SAM parameter is a sort of spectral classification that uses an n-

dimensions angle to match pixels to reference spectra. The algorithm determines the

spectral similarity between two spectra by considering them as vectors in the space and

calculating the angle between the spectra. The angle between the vectors is compared

with each pixel vector with n -dimensions in the space. Smallest angles represent

matches to the reference spectrum and are classified with the desired false pixel color.

The rest of pixels distant from the specified maximum angle threshold (in radians) are

not classified in the mapping image appearing as black pixels. To determine the

localization of the recognized spectra the pixels mapped were overlaid with the DFI (see

Figure S19). The table in Figure S20 represents the number of pixels mapped per

polymer-coated Au/CuS NPs in extracellular and intracellular conditions, showing a

much higher quantity of pixels recognized for the particles exposed to pH 4 than for the

extracellular conditions. The percentage of pixels mapped per cell is also calculated from

the 1-14 ROIs related to the cells in the HDC (Figure S20A) to see the mapping

distribution considering the two different particle populations. The pixels related to the

background were subtracted from the total of pixels present in an HDC, for the

calculation of the percentage of pixels mapped per cell. It is worthy to remark that as

we mentioned before, one bright spot in the DFI can be composed by different number

of pixels, therefore, each pixel mapped in the DFI does not correspond to a single particle.

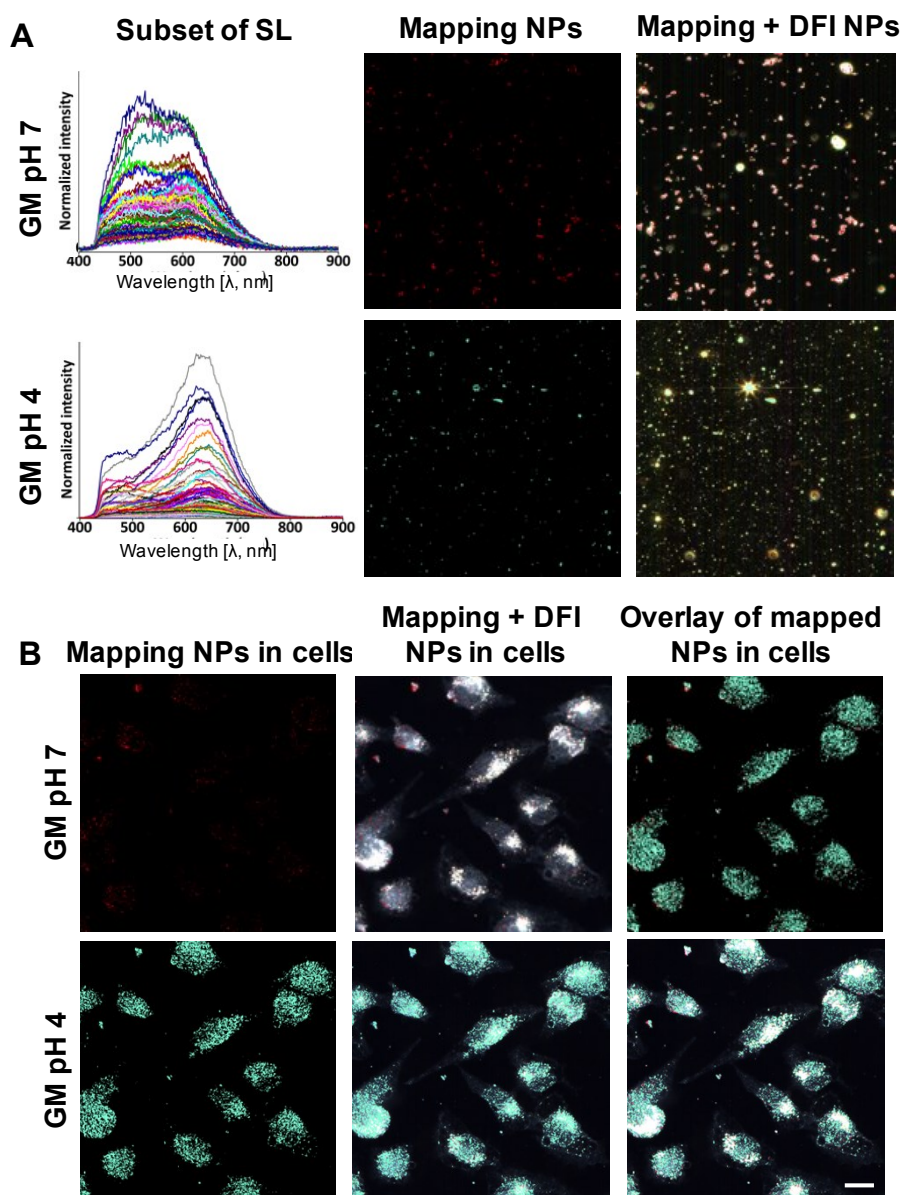
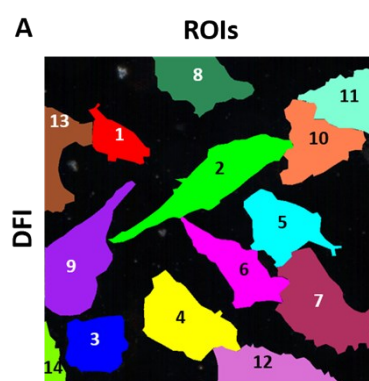


Figure S19. Spectral mapping of polymer-coated Au/CuS NPs exposed to intracellular and extracellular pH conditions. (A) SL subsets of the particles exposed to extracellular (GM pH 7) and intracellular (GM pH 4) used for the spectral mapping procedure (left column). Mapping images of the extracellular (red pixels) and intracellular (blue pixels) SL of the particles in the HDCs of polymer-coated Au/CuS NPs where the spectra were extracted from (middle column). The overlay of the mapping and the DFI is also presented (right column); (B) Mapping images of the extracellular and intracellular SL of the particles in HDCs of the breast cancer cells exposed to polymer-coated Au/CuS NPs for 3 h (left column). The overlay of the mapping and the DFI is shown in the middle column. The right column presents the overlay of the extracellular and intracellular particle pixels mapped (top) and the overlay of the mappings with the DFI (bottom). Scale bar of the images: 10 μ M.



B

Cells (ROIs)	GM pH 7			GM pH 4		
	Nº of pixels mapped	Total nº of pixels	% of cell pixels mapped	Nº of pixels mapped	Total nº of pixels	% of cell pixels mapped
1	345	8035	4.3	2093	8035	26.0
2	232	23696	1.0	3675	23696	15.5
3	337	12832	2.6	2578	12832	20.1
4	111	21537	0.5	2509	21537	11.6
5	99	16563	0.6	1907	16563	11.5
6	171	15562	1.1	1880	15562	12.1
7	229	25598	0.9	3028	25598	11.8
8	417	15948	2.6	4388	15948	27.5
9	472	23562	2.0	6115	23562	26.0
10	141	17560	0.8	3305	17560	18.8
11	259	14333	1.8	3959	14333	27.6
12	109	17309	0.6	1998	17309	11.5
13	212	11557	1.8	1552	11557	13.4
14	58	3806	1.5	786	3806	20.7
Total	3192	227898		39773	227898	

Figure S20. Cell identification and percentage of extracellular and intracellular particle pixels mapped per cell. (A) Cells individually labelled with different false-coloured ROIs and identified with numbers from 1 to 14. (B) Table with the percentage of pixels mapped per cell for polymer-coated Au/CuS NPs exposed to extracellular (GM pH 7) and intracellular (GM pH 4) conditions. Number of pixels mapped per cell (right column), total number of pixels per cell (middle column) and percentage of pixels mapped (right column). The different numbered cells refer to ROIs depicted in Figure A.

3. Verification of the mapping procedure in control cells.

To verify that the spectra mapped in the experimental HDC belong to the polymer-coated Au/CuS NPs, the same SL and SAM conditions used for the mappings of NPs at neutral and acidic pH GM, were mapped against the MDA-MB-231 control cells. Figure S21A shows that no spectra were matched with the spectral data of control cells, verifying that all the spectra found in the mappings corresponded to the spectral of polymer-coated Au/CuS NPs. For further details we provide the cell mean (in Figure S21B) and single spectral profiles (Figure S21C). The mean was calculated from the mean of all the pixels contained in the ROI (inset) delimited by the dashed square in the DFIs.

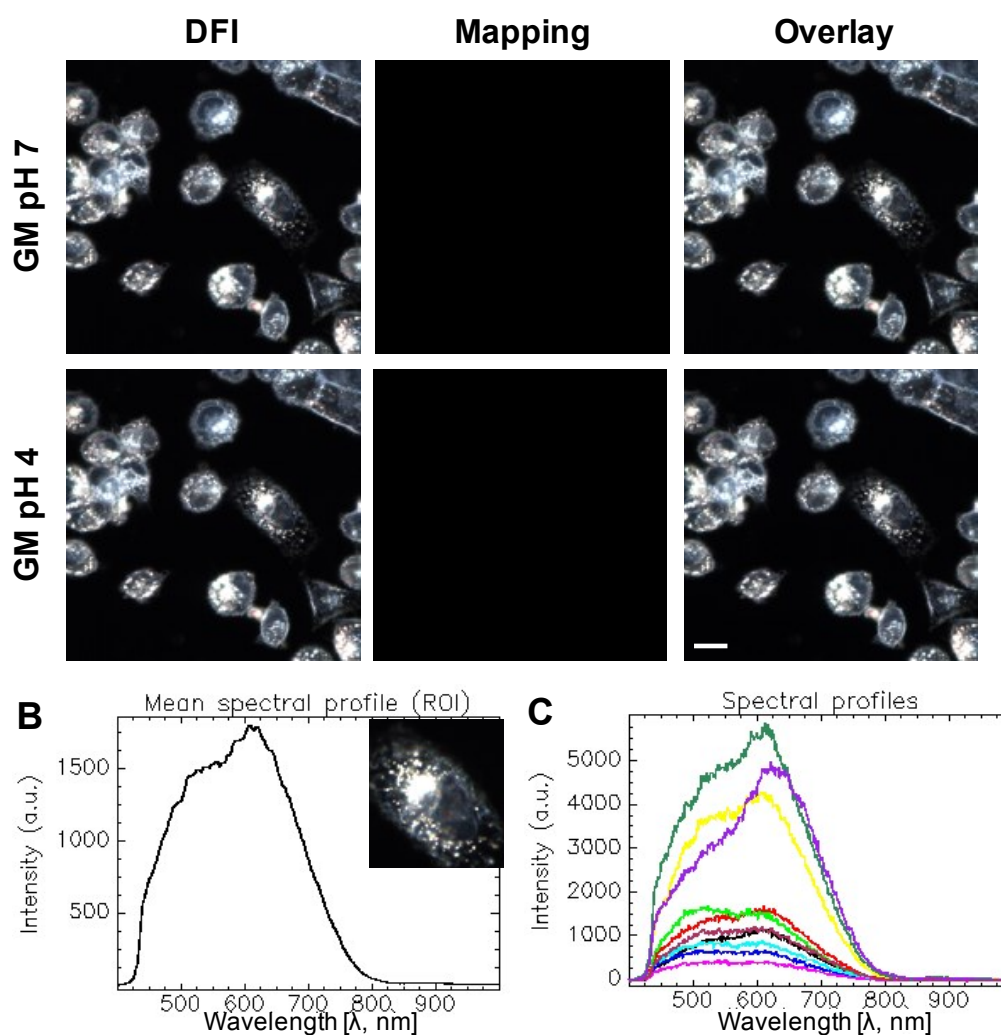


Figure S21. Verification of the origin of the spectra mapped in the HDC of cells without polymer-coated Au/CuS NPs. (A) Mapping of the SLs of NPs exposed to extracellular/early endosome (top row) and lysosomal (bottom row) conditions in the HDC of cells without NPs; Scale bar: 10 μ M; (B) Mean spectral profile of the pixels included in the ROI analysed; The inset corresponds to the ROI delimited by the dotted square in Figure A; (C) Single spectral profiles ($n = 10$) of pixels randomly collected from control cells.

REFERENCES

1. Soliman MG, Pelaz B, Parak WJ, del Pino P. Phase transfer and polymer coating methods toward improving the stability of metallic nanoparticles for biological applications. *Chemistry of Materials*. 2015;27:990–7.
2. Schaadt DM, Feng B, Yu ET. Enhanced semiconductor optical absorption via surface plasmon excitation in metal nanoparticles. *Applied Physics Letters*. 2005;86:063106. doi:10.1063/1.1855423.
3. Lakshmanan SB, Zou X, Hossu M, Ma L, Yang C, Chen W. Local Field Enhanced Au/CuS Nanocomposites as Efficient Photothermal Transducer Agents for Cancer Treatment. *Journal of Biomedical Nanotechnology*. 2012;8:883–90. doi:10.1166/jbn.2012.1486.

4. Schindelin J, Arganda-Carreras I, Frise E, Kaynig V, Longair M, Pietzsch T, et al. Fiji: an open-source platform for biological-image analysis. *Nature Methods*. 2012;9:676–82. doi:10.1038/nmeth.2019.
5. Zamora-Perez P, Tsoutsi D, Xu R, Rivera_Gil P, Zamora-Perez P, Tsoutsi D, et al. Hyperspectral-Enhanced Dark Field Microscopy for Single and Collective Nanoparticle Characterization in Biological Environments. *Materials*. 2018;11:243. doi:10.3390/ma11020243.
6. Kim T, Lee CH, Joo SW, Lee K. Kinetics of gold nanoparticle aggregation: Experiments and modeling. *Journal of Colloid and Interface Science*. 2008;318:238–43.
7. Malikova N, Pastoriza-Santos I, Schierhorn M, Kotov NA, Liz-Marzán LM. Layer-by-layer assembled mixed spherical and planar gold nanoparticles: Control of interparticle interactions. *Langmuir*. 2002;18:3694–7. doi:10.1021/la025563y.